



## Efficient adsorption of Ag(I) and Au(III) on modified magnetic chitosan with amine functionalities

Ahmed M. Donia, Ahmed M. Yousif, Asem A. Atia, Mona F. Elsamalehy\*

*Chemistry Department, Faculty of Science, Menoufia University, Shebin El-Kom, Egypt  
Tel. +20 1227697973; email: mona\_farouk135@yahoo.com*

Received 16 September 2012; Accepted 28 March 2013

---

### ABSTRACT

Sodium tripolyphosphate (TPP) crosslinked magnetic chitosan adsorbent was prepared and immobilized with pentamine moieties. The adsorption behavior of the prepared adsorbent toward Ag(I) and Au(III) was studied at different experimental condition using batch and column methods. The maximum adsorption capacity was found to be 1.7 and 2.3 mmol g<sup>-1</sup> for Ag(I) and Au(III), respectively. The mechanism of interaction between metal ion and adsorbent was found to proceed via complex formation and/or ion exchange. Kinetics and thermodynamic studies showed that the adsorption followed pseudo-second order with endothermic nature. The regeneration of the loaded resin was performed using 1.0M acidified thiourea and was found to be 95–97%. The flow rate of 1.0 mL min<sup>-1</sup> in column experiments was found to be the most preferable rate.

*Keywords:* Adsorption; Magnetic chitosan; Silver; Gold; Kinetics

---

### 1. Introduction

Precious metals are widely used in many fields such as catalysts, electrical and electronic industries, medicine, and jewelry [1]. Because of the increasing industrial need and limited sources of the precious metals, it is necessary to establish an efficient process for their recovery and recycling from different wastewaters. The conventional methods for the removal of metal ions from water and wastewater include oxidation, reduction, precipitation, membrane filtration, ion exchange, and adsorption [1–3]. Extraction of precious metals using solid-phase extractors is one of the most attractive and efficient method [3–5]. Recently, we reported on the use of magnetic resins for the separation of Ag(I) and Au(III) from an aqueous solution

[5–9]. The studied magnetic resins are characterized by ease separation from loading medium using external magnetic field as well as higher uptake. From the economical point of view; much attention has been paid to the low-cost adsorbents. Chitosan has already been described as a suitable low-cost biosorbent for the collection of metal ions [10,11]. The high content of nitrogen atoms in chitosan allows uptake of several metal ions through various mechanisms such as chelation, electrostatic attraction or ion exchange, depending on the type of metal ion and the pH of the solution [12]. Several reports on the modified chitosan with different crosslinkers and different chelating agents have been cited [13–19]. Crosslinked chitosan with water-soluble tripolyphosphate (TPP) or carboxylic acids were also used for removal of metal ions [19–23]. Literature survey indicates that no work has

---

\*Corresponding author.

been done on the magnetic form of TPP crosslinked chitosan. In the present work, the objective is to prepare a magnetic durable low-cost biosorbent for Ag(I) and Au(III) recovery. For these purposes, magnetic chitosan with TPP crosslinker was prepared and immobilized with pentamine moiety. The adsorption behaviour of the adsorbent obtained toward Ag(I) and Au(III) was studied using batch and column techniques. Magnetic properties for the studied resin make it easier to be collected from its sorption medium after batch experiments. Kinetics and thermodynamic parameters of the adsorption process were calculated. The regeneration of the loaded adsorbent was also studied.

## 2. Experimental

### 2.1. Chemicals

Chitosan, sodium TPP, tetraethylenepentamine (TEPA), epichlorohydrin, ferric chloride, and ferrous sulfate were Aldrich products. Metallic gold dissolved in aqua regia and silver nitrate were used as a source for Au(III) and Ag(I), respectively. All other chemicals were Prolabo products and were used as received.

### 2.2. Instruments

Infrared spectra were performed in KBr discs using Nexeus-Nicolite-640 MSA FT-IR, Thermo-electronics Co., New Jersey, USA.

### 2.3. Preparation of magnetite

Magnetite was prepared using the modified Massart method [24]. A 250 mL (0.2 M) FeCl<sub>3</sub> solution was mixed with 250 mL (1.2 M) of FeSO<sub>4</sub> solution. A 200 mL (1.5 M) NH<sub>4</sub>OH solution was added to the above solution of FeCl<sub>3</sub>/FeSO<sub>4</sub> under vigorous stirring. A black precipitate was formed which was allowed to crystallize for another 30 min under magnetic stirring. The precipitate was filtered off and washed with deoxygenated water through magnetic decantation until the pH of the suspension was below 7.5.

### 2.4. Preparation of amine-loaded crosslinked magnetic chitosan

The preparation takes place through three subsequent steps:

#### 2.4.1. Preparation of crosslinked magnetic chitosan gel

Three grams of chitosan was dissolved in 100 mL of dilute acetic acid (5% v/v) to produce the chitosan solution. One gram of magnetite was added to chitosan solution and stirred. Sodium TPP solution (4.0% wt/v) was prepared by dissolving one gram of TPP in 25 mL of deionized water and was adjusted to pH=4 using 1.0 M hydrochloric acid. The TPP solution was dropped through a burette into the above chitosan solution with vigorous stirring. A gelatinous product was obtained and stored in the solution overnight before filtration to give homogenous and well-dispersed chitosan particles [20]. The gel obtained was filtered off and washed several times with deionized water and left to dry. The dried product obtained was then ground and sieved.

#### 2.4.2. Reaction with epichlorohydrine

Two grams of crosslinked chitosan obtained in the above step was suspended in 50 mL of 1.0 N sodium hydroxide, and then, 6 mL of epichlorohydrine dissolved in 50 mL of acetone/water (1:1 v/v) solution was added. The above mixture was stirred for 6 h at 50°C in a water bath. The solid product obtained was filtered off and washed several times with water followed by ethanol.

#### 2.4.3. Immobilization of tetraethylenepentamine

Two grams of the product obtained in the step (ii) was suspended in 100 mL of ethanol/water (1/1 v/v), and then, 6 mL of TEPA was added. The reaction mixture was stirred at 60°C for 12 h. The product obtained was filtered off, washed with water followed by ethanol and then dried in air.

The concentration of amino groups in the obtained resin was estimated using a volumetric method [7]. Forty milliliters of 0.05 N HCl solution was added to 0.1 g resin and conditioned for 15 h on a shaker. The number of moles of HCl was measured through the titration against 0.05 N NaOH solution and phenolphthalein as an indicator. The number of moles of HCl interacting with the amino groups was calculated, and then, the amino group concentration (in mmol g<sup>-1</sup> of resin) was calculated using the following equation:

Concentration of amino groups

$$= \frac{(M_1 - M_2) \times 40}{0.1} \text{ mmol/g of resin} \quad (1)$$

where  $M_1$  and  $M_2$  are the initial and final concentration of HCl, respectively.

### 2.5. Preparation of solutions

A stock solution of gold ( $1.4 \times 10^{-2}$  M) was prepared by dissolving metallic gold in an aqua regia mixture ( $\text{HNO}_3:\text{HCl}$ , 1:3 v/v). A stock solution of the silver nitrate ( $1.4 \times 10^{-2}$  M) was also prepared by dissolving  $\text{AgNO}_3$  in distilled water. Working solutions were prepared by dilution of a stock solutions to the desired concentration using distilled water. A stock solution of EDTA ( $5 \times 10^{-3}$  M) was prepared and standardized against a solution of ( $1 \times 10^{-2}$  M)  $\text{MgSO}_4 \cdot 7\text{H}_2\text{O}$  using Eriochrome Black-T (EBT) as an indicator.  $\text{HNO}_3$  and NaOH solutions were used to obtain the desired pH of the medium. Thiourea (1.0 M) acidified by  $\text{H}_2\text{SO}_4$  (0.1 M) was used as an eluent for stripping Ag(I) and Au(III) adsorbed.

### 2.6. Adsorption studies using batch technique

#### 2.6.1. Effect of pH

Adsorption of Ag(I) and Au(III) on resin under controlled pH was carried out by swelling 0.1 g of dry adsorbent in a number of flasks containing 50 mL of distilled water for 1 h. Fifty milliliters of metal ions solution ( $1.4 \times 10^{-2}$  M) was added to the flasks where the initial concentration of the metal ions became ( $7 \times 10^{-3}$  M). The desired pH was obtained using  $\text{HNO}_3$  and NaOH. The flasks were shaken for 3 h on a Vibromatic-384 shaker at 300 rpm and at  $28 \pm 1^\circ\text{C}$  on a Vibromatic-384 shaker. Studying the adsorption of Ag (I) or Au(III) in strong basic media was avoided due to the precipitation of metal hydroxide.

After conditioning, the supernatant of each flask was analyzed for Ag(I) and Au(III) using compleximetric titration with EDTA by the replacement titration method using potassium tetracyanonickelate(II) [25]. The released Ni(II) ions were determined. Direct titration with murexide indicator was used in the case of Ag(I), whereas back titration with EBT indicator was used in the case of Au(III).

#### 2.6.2. Effect of contact time

The effect of contact time on the uptake of Ag(I) and Au(III) by resin was carried out by swelling 0.1 g of dry resin in a number of flasks containing 50 mL of distilled water for 1 h. Fifty milliliters of metal ions solution ( $1.4 \times 10^{-2}$  M) was added to the flask where the initial concentration of the metal ions became ( $7 \times 10^{-3}$  M), and the pH of the solution was 6.9 and

0.5 for Ag(I) and Au(III), respectively. The contents of the flask were shaken on a Vibromatic-384 shaker at 300 rpm and  $28 \pm 1^\circ\text{C}$ . Five milliliters was taken from the flasks at different time intervals where the residual concentration of the metal ions was determined following the above method.

#### 2.6.3. Adsorption isotherms

Complete adsorption isotherms for Ag(I) and Au (III) were obtained by soaking 0.1 g of dry resin in a series of flasks each containing 50 mL of distilled water for 1 h. To each flask, 50 mL of Ag(I) and Au (III) ions at the desired concentration were added. The initial pH of solutions was 6.9 and 0.5 for Ag(I) and Au(III), respectively. The flasks were shaken at 300 rpm while keeping the temperature at 30, 45, or  $55^\circ\text{C}$  for 3 h. Later on, the residual concentration was determined where the metal ion uptake was calculated.

### 2.7. Adsorption studies using column technique

Column experiments were performed in a plastic column with a length of 10 cm and a diameter of 1 cm. A small amount of glass wool was placed at the bottom of the column to keep the contents. A known quantity of the resin was placed in the column to yield bed height of 0.3, 0.75, or 1.5 cm. Metal ion solution having the desired initial concentration (initial pH of solutions was 6.9 and 0.5 for Ag(I) and Au(III), respectively) was flowed downward through the column using flow rates of 1, 2 or  $3 \text{ mL min}^{-1}$ . Samples were collected from the outlet of the column at different time intervals and analyzed for metal ion concentration. The operation of the column was terminated when the outlet metal ion concentration matched its initial concentration. The outlet metal ion concentrations at different time intervals over initial concentration ( $C_t/C_o$ ) values were plotted versus time at different flow rates to give the breakthrough curves.

### 2.8. Regeneration experiments

Regeneration experiments were performed by equilibrating 0.1 g of adsorbent with 100 mL of metal ion solution ( $7 \times 10^{-3}$  M), and pH of solutions was 6.9 and 0.5 for Ag(I) and Au(III), respectively, for 3 h, and the total uptake was estimated. Then, the solution was decanted, and the adsorbent was washed thoroughly with distilled water. The loaded adsorbent was

equilibrated for 3 h in 100 mL of thiourea (1.0 M) acidified with H<sub>2</sub>SO<sub>4</sub> (0.1 M). After elution, the adsorbent was carefully washed with distilled water for reuse in the second uptake run. The efficiency of regeneration was calculated by dividing the total adsorption capacity in the second run by that of the first one.

### 3. Results and discussion

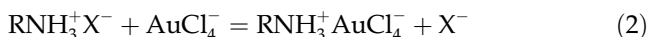
The preparation of the investigated resin is represented in Fig. 1. The ionic interaction between the protonated amino groups in chitosan (positively charged) and negatively charged crosslinker ion (TPP) at pH=4 has been reported [20]. Resin was obtained by successive addition of epichlorohydrin and TEPA. The investigated adsorbent displays a good durability against soaking in 0.5 M HCl and 0.1 M NaOH for 24 h without any significant activity loss. The amine active sites concentration of resin was found to be 6.4 mmol g<sup>-1</sup>.

Fig. 2(b) shows the IR spectra of resin. The spectrum displays bands at 1,200 and 1,520 cm<sup>-1</sup> (not found in Fig. 2(a)). These bands were assigned to  $\nu$  P=O and  $\nu$  -NH<sub>3</sub><sup>+</sup>, respectively. The observed band at 840 cm<sup>-1</sup> corresponds to -NH of the secondary amine for bending vibration. These findings confirm the success of modification [20].

#### 3.1. Batch method

##### 3.1.1. Effect of pH

The effect of the acidity of the medium on the uptake of Ag(I) and Au(III) was shown in Fig. 3. It is seen that the uptake of Ag(I) increases as the pH increases till reaching a maximum value at pH=6. This behavior indicates the complex formation mechanism between Ag(I) and the donor atoms (N) on the adsorbent [3–5]. For Au(III), in acidic medium and in the presence of high concentration of Cl<sup>-</sup>, AuCl<sub>4</sub><sup>-</sup> became the predominant species so the interaction proceeded between this species ion and the protonated sites of the adsorbent through ion exchange mechanism [4,26].



##### 3.1.2. Kinetic studies

Fig. 4 shows the change in the uptake of Ag(I) and Au(III) by the adsorbent as a function of time at initial concentration of  $7 \times 10^{-3}$  M. For both metal ions, the acidity of the medium was adjusted at pH=6.9 (natural) and 0.5 for Ag(I) and Au(III), respectively.

Obviously, the equilibrium time for the uptake of Ag(I) and Au(III) reached within 60 min. The uptake-time data obtained were treated in the form of two simplified kinetic models including pseudo-first order and pseudo-second order. The pseudo-first-order model is expressed as [27]:

$$\log(q_e - q_t) = \log q_e - \left(\frac{k_1}{2.303}\right)t \quad (3)$$

where  $k_1$  is the pseudo-first-order rate constant (min<sup>-1</sup>) of adsorption, and  $q_e$  and  $q_t$  (mmol g<sup>-1</sup>) are the amounts of metal ion adsorbed at equilibrium and time  $t$  (min), respectively. On the other hand, the pseudo-second-order model is expressed as [28]:

$$\frac{t}{q_t} = \frac{1}{k_2 q_e^2} + \left(\frac{1}{q_e}\right)t \quad (4)$$

where  $k_2$  is the pseudo-second-order rate constant of adsorption (g mmol<sup>-1</sup> min<sup>-1</sup>). The kinetic parameters for the pseudo-first- and pseudo-second-order models are determined from the linear plots of  $\log(q_e - q_t)$  versus  $t$  or  $(t/q_t)$  versus  $t$ , respectively. The validity of each model could be checked by the fitness of the straight lines ( $R^2$  values). Accordingly as shown in Table 1, the adsorption of Ag(I) and Au(III) on the adsorbent is perfectly fit pseudo-second-order model rather than pseudo-first order one. In addition, the experimental and theoretical values of  $q_e$  (obtained from pseudo-second-order model) are closely similar, confirming the validity of that model to the adsorption system under consideration. This implies that the rate-determining step of the adsorption reaction depends on both the concentration of the active sites and the textural properties of the resin.

The adsorption takes place through multistep mechanism including: (i) external film diffusion; (ii) intraparticle diffusion and (iii) interaction between adsorbate and active site [29,30].

$$q_t = K_i t^{0.5} + X \quad (5)$$

where  $q_t$  is the amounts of metal ion adsorbed at time  $t$ ,  $K_i$  is the intraparticle diffusion rate constant (mmol g<sup>-1</sup> min<sup>0.5</sup>), and  $X$  is the intercept of the straight line which is proportional to the boundary layer thickness. Fig. 5 shows the plots of  $q_t$  versus  $t^{0.5}$  for Ag(I) and Au(III) on resin. The plot of Ag(I) displays a straight line with positive intercept to Y-axis. This suggests that the rate of adsorption is controlled by intraparticle diffusion as well as boundary layer thickness [31–33]. The plot of Au(III) displays two straight line

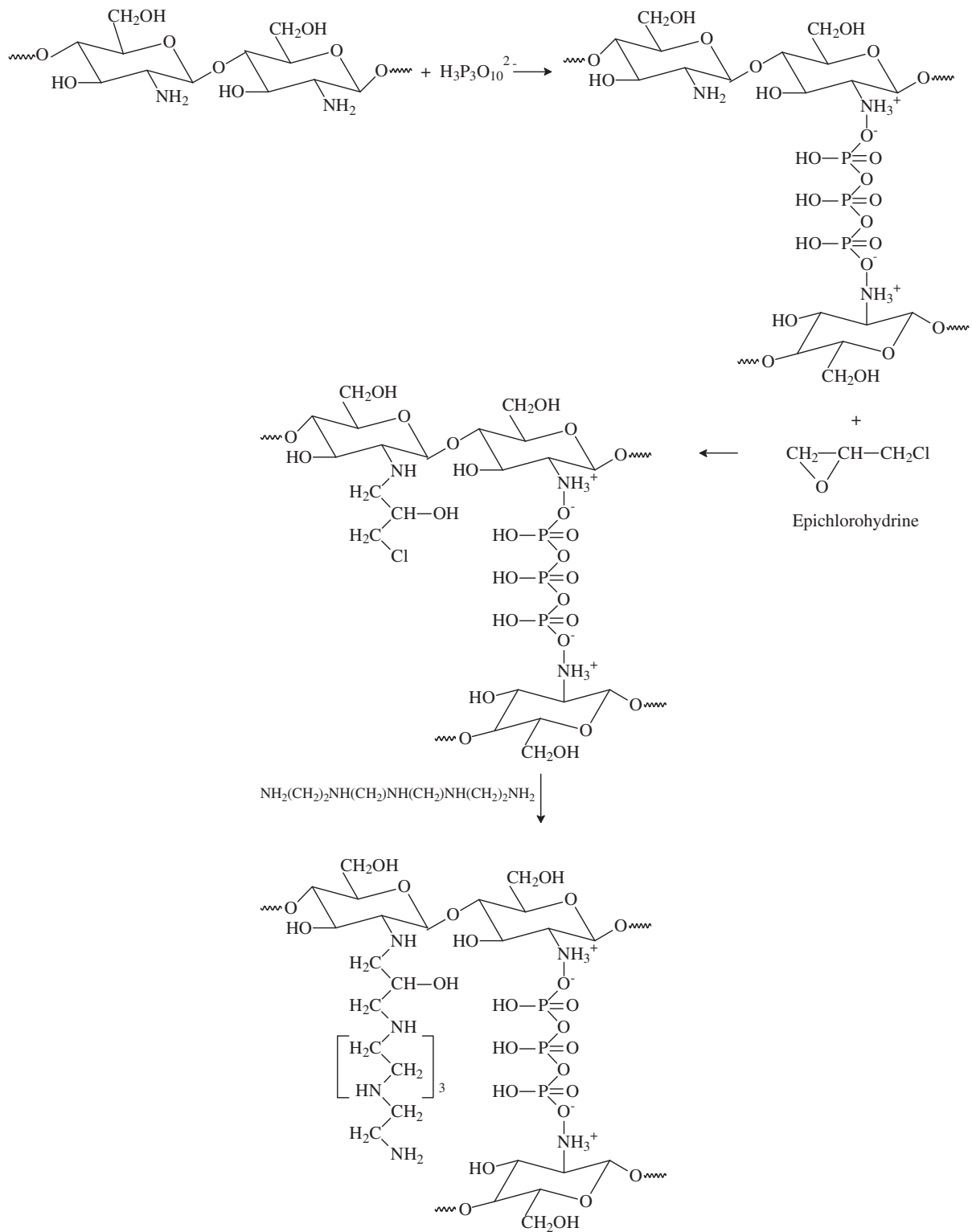


Fig. 1. Suggested reaction route of resin synthesis.

regions. In region I, the straight line passes through the origin indicating that the rate is initially controlled by intraparticle diffusion [31–33]. In region II, the

positive values of  $X$  obtained after extrapolation of the line indicates that the rate is mainly controlled by boundary layer diffusion [8,34,35].

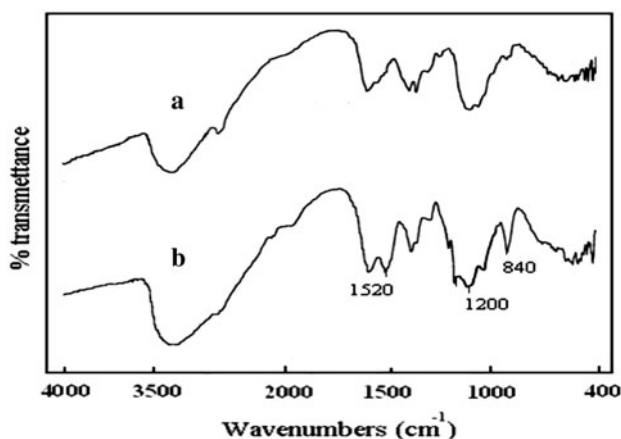


Fig. 2. Infrared spectrum of resin; (a) before modification and (b) after modification.

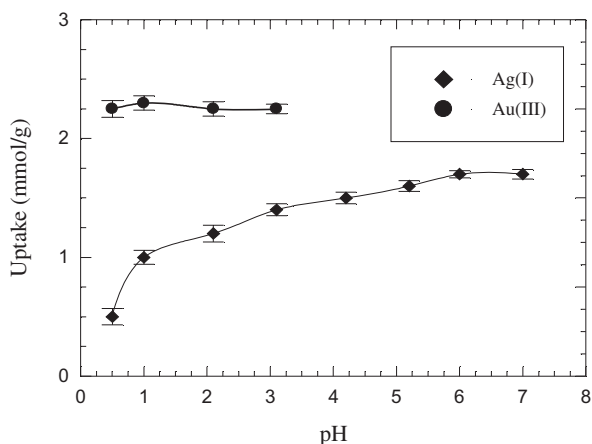


Fig. 3. Effect of pH on the adsorption of Ag(I) and Au(III) on resin at initial concentrations of  $7 \times 10^{-3}$  M and at 28°C.

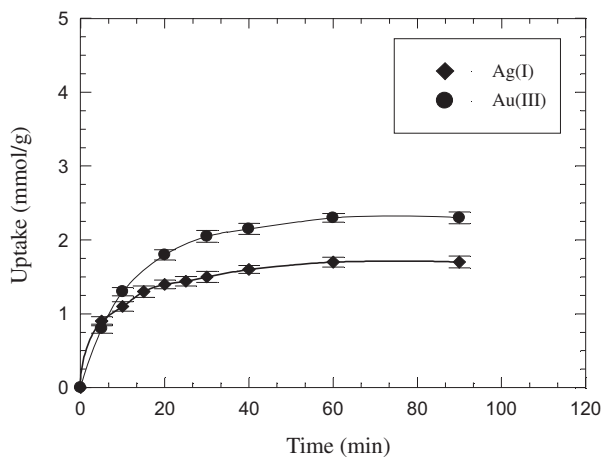


Fig. 4. Effect of time on the adsorption of Ag(I) and Au(III) on resin at initial concentration  $7 \times 10^{-3}$  M and at 28°C.

### 3.1.3. Adsorption isotherms

Fig. 6 shows the adsorption isotherms of Ag(I) and Au(III) on resin at different temperatures. The adsorption curves show maximum uptake values for Ag(I) and Au(III) at 1.7 and 2.3 mmol g<sup>-1</sup> at 30°C, respectively. These values are comparable with the values reported by others in Table 2 but with faster kinetics [1–3,40]. These values increase as the temperature increases. The adsorption data were plotted according to Langmuir equation [5–9].

$$\frac{C_e}{q_e} = \frac{C_e}{Q_{\max}} + \frac{1}{K_L Q_{\max}} \quad (6)$$

where  $C_e$  is the equilibrium concentration of metal ions in solution (mmol L<sup>-1</sup>),  $q_e$  is the adsorbed amount of metal ions at equilibrium concentration (mmol g<sup>-1</sup>),  $Q_{\max}$  is the maximum adsorption capacity (mmol g<sup>-1</sup>), and  $K_L$  is the Langmuir binding constant which is related to the energy of adsorption (L mmol<sup>-1</sup>). Plotting  $C_e/q_e$  against  $C_e$  gives a straight line with slope and intercept equal to  $1/Q_{\max}$  and  $1/K_L Q_{\max}$ , respectively. The values of  $K_L$  and  $Q_{\max}$  at different temperatures for adsorption of Ag(I) and Au(III) were calculated and reported in Table 3. It is seen that the value of  $Q_{\max}$  (obtained from Langmuir plots) at 30°C is mainly consistent with that experimentally obtained, indicating that the adsorption process is mainly proceeding through monolayer coverage. It is also seen that Au(III) displays a higher  $K_L$  values than Ag(I). This may be related to the stronger electrostatic attraction between  $\text{AuCl}_4^-$  and adsorbent than complex formation in the case of Ag(I).

The degree of suitability of adsorbent toward metal ions was estimated from the values of separation factor constant ( $R_L$ ), which gives indication for the possibility of the adsorption process to proceed.  $R_L > 1.0$  unsuitable;  $R_L = 1$  linear;  $0 < R_L < 1$  suitable;  $R_L = 0$  irreversible [27]. The value of  $R_L$  could be calculated from the relation

$$R_L = \frac{1}{1 + K_L C_o} \quad (7)$$

where  $K_L$  (L mmol<sup>-1</sup>) is the Langmuir equilibrium constant, and  $C_o$  (mmol L<sup>-1</sup>) is the initial concentration of metal ion. The value of  $R_L$  at initial concentration and at 30°C are 0.165 and 0.097 for Ag(I) and Au(III), respectively, indicating the suitability of the adsorbent for the adsorption of Ag(I) and Au(III) from their aqueous solutions.

Table 1  
Parameters of pseudo-first- and pseudo-second-order models for the adsorption of Ag(I) and Au(III) on resin

Resin	$q_e^{exp.}$ (mmol g <sup>-1</sup> )	Pseudo-first order			Pseudo-second order		
		$k_1$ (min <sup>-1</sup> )	$q_e^{calc.*}$ (mmol g <sup>-1</sup> )	$R^2$	$k_2$ (g mmol <sup>-1</sup> min <sup>-1</sup> )	$q_e^{calc.**}$ (mmol g <sup>-1</sup> )	$R^2$
Ag(I)	1.7	0.057	1.03	0.98	0.093	1.8	0.99
Au(III)	2.3	0.042	1.5	0.87	0.090	2.4	0.98

\*Calculated from pseudo-first-order model.

\*\*Calculated from pseudo-second-order model.

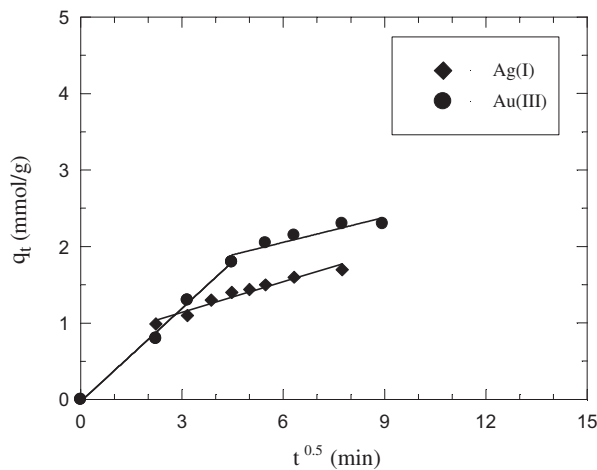


Fig. 5. The intraparticle diffusion kinetic model of the adsorption of Ag(I) and Au(III) on resin at initial concentrations of  $7 \times 10^{-3}$  M and at 28°C.

### 3.1.4. Thermodynamic studies

The values of  $K_L$  at different temperatures were treated according to Van't Hoff equation [36]

$$\ln K_L = \frac{-\Delta H^\circ}{RT} + \frac{\Delta S^\circ}{R} \quad (8)$$

where  $\Delta H^\circ$  (J mol<sup>-1</sup>) and  $\Delta S^\circ$  (J mol<sup>-1</sup> K<sup>-1</sup>) are enthalpy and entropy changes, respectively,  $R$  is the universal gas constant (8.314 J mol<sup>-1</sup> K<sup>-1</sup>), and  $T$  is the absolute temperature (in Kelvin). Plotting  $\ln K_L$  against  $1/T$  gives a straight line with slope and intercept equal to  $\Delta H^\circ/R$  and  $\Delta S^\circ/R$ , respectively. The observed increase in both values of  $Q_{max}$  and  $K_L$  at elevated temperature indicates the endothermic nature of the adsorption process. Plotting  $\ln K_L$  against  $1/T$  gives a straight line with slope and intercept equal to  $\Delta H^\circ/R$  and  $\Delta S^\circ/R$ , respectively. The values of  $\Delta H^\circ$  and  $\Delta S^\circ$  were calculated and reported in Table 4. The positive values of  $\Delta S^\circ$  may be related to the liberation of water of hydration during the adsorption process

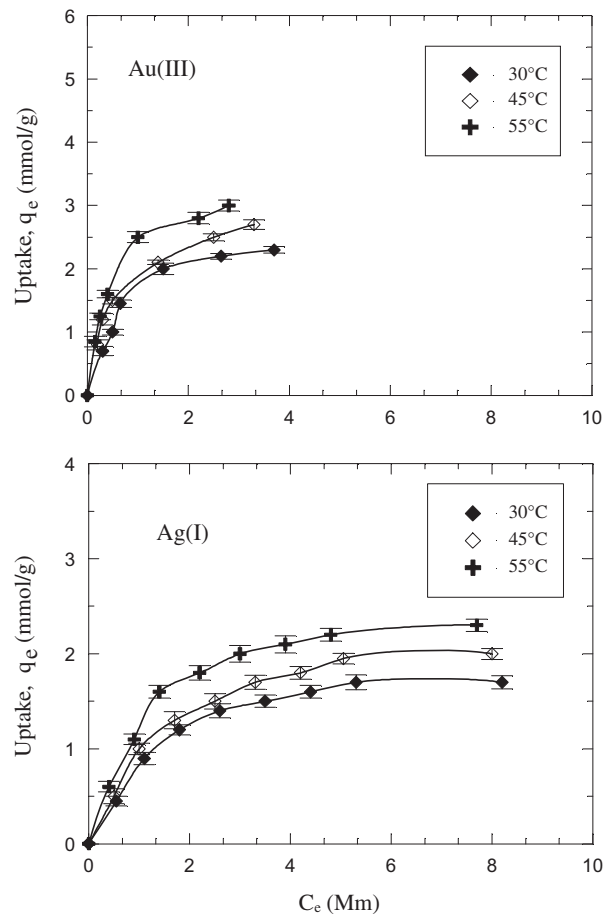


Fig. 6. Adsorption isotherms of Ag(I) and Au(III) on resin at different temperatures.

causing the increase in the randomness of the system [37,38]. The positive values of  $\Delta H^\circ$  indicate an endothermic nature for the uptake process. The observed greater positive value of  $\Delta S^\circ$  for Au(III) than that of Ag(I) may be related to the mechanism of interaction between metal ion and active sites. The chelation mechanism for Ag(I) with active sites gives more ordered form than electrostatic attraction mechanism

Table 2  
Comparative study of the adsorption capacity and equilibrium time for the investigated resins

Adsorbent	Uptake (mmol/g)		Eq. time (min)		Reference
	Ag(I)	Au(III)	Ag(I)	Au(III)	
Crosslinked chitosan-glycine	–	0.08	–	180	[1]
Modified chitosan-L-lysine	–	0.06	–	300	[2]
Modified chitosan-thiourea	3.20	–	180	–	[3]
Modified chitosan-thiourea/glutaraldehyde	1.50	3.50	80	90	[40]
Resin	1.70	2.30	60	60	This work

for Au(III) adsorption. Another explanation may be discussed through the chelation mechanism through directional coordinate bonds for Ag(I) which may give controlled monolayer adsorption, whereas ion pair mechanism through nondirectional electrostatic attraction for  $\text{AuCl}_4^-$  may give a less controlled monolayer formation. Gibbs free energy of adsorption ( $\Delta G^\circ$ ) was calculated from the following relation [38]:

$$\Delta G^\circ = \Delta H^\circ - T\Delta S^\circ \quad (9)$$

The values of  $\Delta G^\circ$  at different temperatures were calculated and reported in Table 4. The negative values of  $\Delta G^\circ$  indicate that the adsorption reaction is spontaneous. The observed increase in negative values of  $\Delta G^\circ$  with increasing temperature implies that the adsorption becomes more favorable at higher temperatures [39].

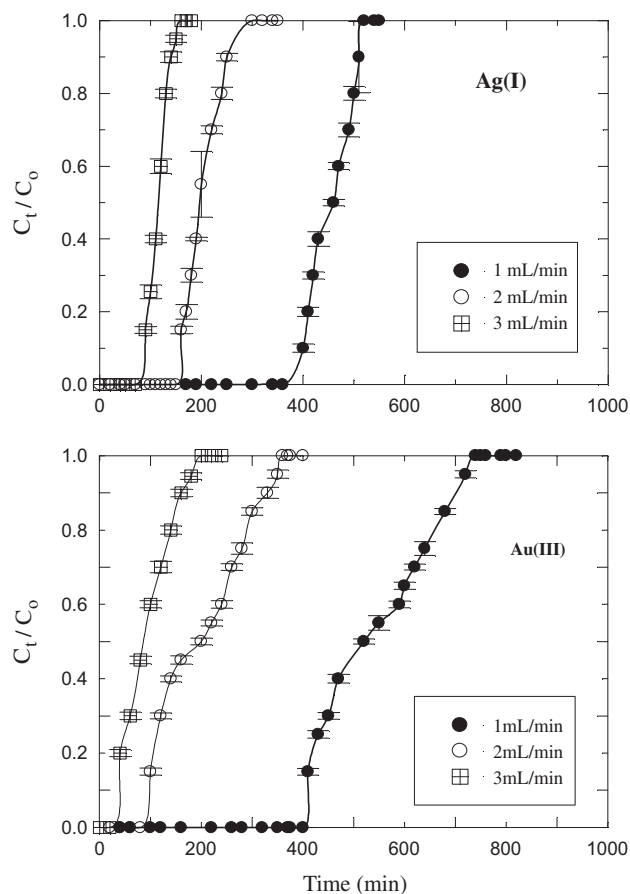


Fig. 7. Effect of flow rate on the uptake of Ag(I) (pH=6.9) and Au(III) (pH=0.5) on resin at a fixed bed height of 1.5 cm.

### 3.2. Column method

#### 3.2.1. Effect of flow rate

The breakthrough curves of the uptake of Ag(I) and Au(III) by the adsorbent at different flow rates (1, 2, and 3 mL min<sup>-1</sup>) and a fixed bed height of 1.5 cm are shown in Fig. 7 and Table 5. Obviously, the breakthrough and exhaustion of the resin occurs faster at higher flow rates. Also as the flow rate increases, the metal ions appear in the effluent rapidly resulting in much sharper breakthrough curves. This behavior may be attributed to the insufficient residence time of the metal ions on the column, which negatively affects the interaction process as well as the diffusion of metal ions through the pores of the adsorbent [40]. It is also seen that, for all flow rates, Au(III) displays longer breakthrough time than that of Ag(I). This indicates the efficient interaction of Au(III) (as  $\text{AuCl}_4^-$ ) relative to complex formation interaction of Ag(I).

#### 3.2.2. Effect of bed height

As shown in Fig. 8 and Table 5, the bed height was varied from 0.3 to 1.5 cm while the flow rate was held constant at 1 mL min<sup>-1</sup>. The influence of bed height was well checked in terms of breakthrough time ( $t_b$ ) and service time ( $t_s$ ). Both parameters ( $t_b$ ) and ( $t_s$ ) were increased by increasing the bed height. Generally, the removal efficiency of the adsorbent was significantly affected by the bed height and found to

Table 3  
Langmuir constants for the adsorption of Ag(I) and Au(III) on resin

Temperature (°C)	Ag(I)				Au(III)			
	$q_e^{exp.}$ (mmol g <sup>-1</sup> )	$Q_{max}^*$ (mmol g <sup>-1</sup> )	$K_L$ (L mmol <sup>-1</sup> )	$R^2$	$q_e^{exp.}$ (mmol g <sup>-1</sup> )	$Q_{max}^*$ (mmol g <sup>-1</sup> )	$K_L$ (L mmol <sup>-1</sup> )	$R^2$
30	1.7	2.0	0.720	0.9877	2.3	2.8	1.315	0.9898
45	2.1	2.4	0.649	0.9958	2.7	3.0	1.759	0.9935
55	2.3	2.6	0.945	0.9909	3.2	3.6	2.059	0.9956

\*Calculated from Langmuir model plotting.

Table 4  
Thermodynamic parameters for the adsorption of Ag(I) and Au(III) on resin at different temperatures

Temperature (K)	Ag(I)				Au(III)			
	$\Delta G^\circ$ (kJ mol <sup>-1</sup> )	$\Delta H^\circ$ (kJ mol <sup>-1</sup> )	$\Delta S^\circ$ (J mol <sup>-1</sup> K <sup>-1</sup> )	$T\Delta S^\circ$ (kJ mol <sup>-1</sup> )	$\Delta G^\circ$ (kJ mol <sup>-1</sup> )	$\Delta H^\circ$ (kJ mol <sup>-1</sup> )	$\Delta S^\circ$ (J mol <sup>-1</sup> K <sup>-1</sup> )	$T\Delta S^\circ$ (kJ mol <sup>-1</sup> )
305	-16.20	11.64	91.28	27.84	-17.81	18.29	118.99	36.10
320	-17.56			29.20	-19.59			37.88
330	-18.48			30.12	-20.77			39.06

be directly proportional to it. Bed depth service time model (BDST) is a simple model, in which the bed height ( $Z$ ) and service time ( $t_s$ ) of the column are linearly related as given in the following equation [40]:

$$t_s = \frac{N_o Z}{C_o v} - \frac{1}{K_a C_o} \ln\left(\frac{C_o}{C_t} - 1\right) \quad (10)$$

where  $C_o$  (mmol L<sup>-1</sup>) is the initial metal ion concentration,  $C_t$  (mmol L<sup>-1</sup>) is the metal ion concentration at the service time just before equivalence to the initial concentration ( $C_t/C_o = 99/100$ ),  $N_o$  is the total adsorption capacity (mmol of solute/L of sorbent bed),  $v$  is the linear velocity (cm min<sup>-1</sup>), and  $K_a$  characterizes the rate constant of transfer (L mmol<sup>-1</sup> min<sup>-1</sup>). The values of  $N_o$  and  $K_a$  were calculated from the slope and intercept of the BDST plots, respectively and reported in Table 5. If  $K_a$  is large, even a short bed height will avoid breakthrough, but if  $K_a$  is small a progressively longer bed height is required to avoid breakthrough. The values of for Ag(I) and Au(III) are 57.0 and 82.0 (L mmol<sup>-1</sup> min<sup>-1</sup>), respectively. Again the observed higher  $K_a$  value for Au(III) is related to its stronger nature of interaction with the adsorbent and consistent with its longer breakthrough time than that of Ag(I). The critical bed height ( $Z_o$ ) can be calculated by setting  $t_s = 0$  in Eq. (10) [40].

$$Z_o = \frac{v}{K_a N_o} \ln\left(\frac{C_o}{C_b} - 1\right) \quad (11)$$

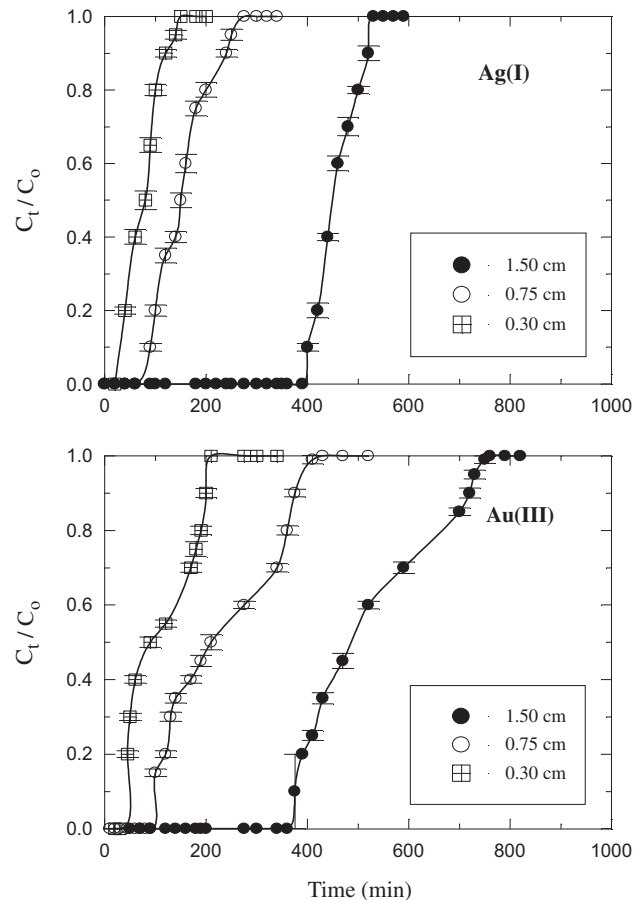


Fig. 8. Effect of bed height on the uptake of Ag(I) (pH=6.9) and Au(III) (pH=0.5) on resin at fixed flow rate of 1 mL min<sup>-1</sup>.

Table 5  
Data of column studies for the uptake of Ag(I) and Au(III) on resin at different flow rates and bed heights

Metal ion	Bed height (cm)	Flow rate (mL min <sup>-1</sup> )	$t_b$ (min)	$t_s$ (min)	$K_a$ (L mmol <sup>-1</sup> min <sup>-1</sup> )	$N_o$ (mmol g <sup>-1</sup> )	$Z_o$ (cm)	$R^2$
Ag(I)	1.5	1	270	520	57	1.60	0.069	0.9987
	1.5	2	100	300				
	1.5	3	90	150				
	0.75	1	90	275				
	0.3	1	40	150				
Au(III)	1.5	1	375	750	82	2.29	0.036	0.9998
	1.5	2	70	370				
	1.5	3	40	200				
	0.75	1	100	410				
	0.3	1	45	210				

where  $C_b$  is the metal ion concentration at the breakthrough point (mmol L<sup>-1</sup>). The above equation implies that  $Z_o$  depends on the kinetics of the sorption process, the residence time of the solute and the sorption capacity of the resin [40]. The critical bed height for Ag(I) and Au(III) columns were calculated and found to be 0.069 and 0.036 cm, respectively.

### 3.3. Regeneration of loaded resins

Sorption/desorption cycles up to five runs were carried out for Ag(I) and Au(III) on resin. The elution of the metal ions was performed using 100 mL of 1.0 M thiourea acidified with drops of 0.1 M H<sub>2</sub>SO<sub>4</sub>.

The efficiency of regeneration was obtained using the following equation

$$\text{Efficiency of regeneration (\%)} = \frac{\text{Total uptake in the second run}}{\text{Total uptake in the first run}} \times 100 \quad (12)$$

Generally, the efficiency of regeneration was found to be 97 and 95% for Ag(I) and Au(III), respectively over five cycles.

## 4. Conclusions

Adsorption of Ag(I) and Au(III) from aqueous solutions was studied using a magnetic adsorbent derived from chemically modified chitosan. The adsorption process was carried out using batch and column methods. The total uptake capacity was found to be 1.7 and 2.3 mmol g<sup>-1</sup> for Ag(I) and Au(III), respectively. Kinetic studies indicated that the

adsorption reaction follows the pseudo-second-order kinetics. Thermodynamic parameters obtained indicated that the adsorption process is spontaneous and endothermic. The mechanism of interaction between metal ion and resin was also clarified. The resin obtained showed a good durability and easy regeneration using 1.0 M thiourea acidified with 0.1 M H<sub>2</sub>SO<sub>4</sub>. Magnetic properties for the studied resin make it easier to be collected from its sorption medium after batch experimental. The regeneration efficiency was found to be 95–97%. The flow rate of 1.0 mL min<sup>-1</sup> in column experiments was found to be the most preferable rate. Column experiments have clearly illustrated that it is applicable to use column technique in the industrial field in order to recover gold and silver ions from their solutions.

## References

- [1] A. Ramesh, H. Hasegawa, W. Sugimoto, T. Maki, K. Ueda, Adsorption of gold(III), platinum(IV) and palladium(II) onto glycine modified crosslinked chitosan resin, *Biores. Technol.* 99 (2008) 3801–3809.
- [2] K. Fujiwara, A. Ramesh, T. Maki, H. Hasegawa, K. Ueda, Adsorption of platinum(IV) and palladium(II) and gold(III) from aqueous solution onto l-lysine modified crosslinked chitosan resin, *J. Hazard Mater.* 146 (2007) 39–50.
- [3] L. Wang, R.G. Xing, S. Liu, H. Yu, Y. Qin, K. Li, J. Feng, R. Li, P. Li, Recovery of silver (I) using a thiourea-modified chitosan resin, *J. Hazard Mater.* 180 (2010) 577–582.
- [4] A.A. Atia, Adsorption of silver(I) and gold(III) on resins derived from bithiourea and application to retrieval of silver ions from processed photo films, *Hydrometallurgy* 80 (2005) 98–106.
- [5] A.M. Donia, A.A. Atia, H.A. El-boraey, D. Mabrouk, Adsorption of Ag(I) on glycidyl methacrylate/N, N-methylene bisacrylamide chelating resins with embedded iron oxide, *Sep. Purif. Technol.* 48 (2006) 281–287.
- [6] A.M. Donia, A.A. Atia, H.A. EL-Boraey, D. Mabrouk, Uptake studies of copper (II) on glycidyl methacrylate chelating resin containing Fe<sub>2</sub>O<sub>3</sub> particles, *Sep. Purif. Technol.* 49 (2006) 64–70.

- [7] A.A. Atia, A.M. Donia, H.A. Awed, Synthesis of magnetic chelating resins functionalized with tetraethylenepentamine for adsorption of molybdate from aqueous solutions, *J. Hazard Mater.* 155 (2008) 13–22.
- [8] A.M. Donia, A.A. Atia, A.M. Heniesh, Efficient removal of Hg(II) using magnetic chelating resin derived from copolymerization of bithiourea/thiourea/glutaraldehyde, *Sep. Purif. Technol.* 60 (2008) 46–53.
- [9] A.A. Atia, A.M. Donia, M.M. Elhawary, Effect of crosslinker type and embedded magnetite on the uptake behaviour of amine containing glycidyl methacrylate resins towards iron(III), *Sep. Sci. Technol.* 43 (2008) 403–419.
- [10] L. Fan, C. Luo, Z. Lv, F. Lu, H. Qiu, Preparation of magnetic modified chitosan and adsorption of  $Zn^{2+}$  from aqueous solutions, *Colloids Surf. B* 88 (2011) 574–581.
- [11] M. Monier, D.A. Abdel-Latif, Preparation of cross-linked magnetic chitosan-phenylthiourea resin for adsorption of Hg(II), Cd(II) and Zn(II) ions from aqueous solutions, *J. Hazard Mater.* 209–210 (2012) 240–249.
- [12] W.S. Wan Ngaha, L.C. Teonga, M.A.K.M. Hanafiah, Adsorption of dyes and heavy metal ions by chitosan composites: A review, *Carbohydr. Polym.* 83 (2011) 1446–1456.
- [13] A.M. Donia, A.M. Yousif, A.A. Atia, M.F. Elsamalehy, Selective separation of  $Hg^{2+}$  on modified crosslinked chitosan beads enriched with amine groups, *Sep. Sci. Technol.* 46 (2011) 1638–1646.
- [14] C. Shen, Y. Shen, Y. Wena, H. Wang, W. Liu, Fast and highly efficient removal of dyes under alkaline conditions using magnetic chitosan-Fe(III) hydrogel, *Water Res.* 45 (2011) 5200–5210.
- [15] H. Yan, L. Yang, Z. Yang, H. Yang, A. Li, R. Cheng, Preparation of chitosan/poly(acrylic acid) magnetic composite microspheres and applications in the removal of copper(II) ions from aqueous solutions, *J. Hazard Mater.* 229–230 (2012) 371–380.
- [16] V.K. Mourya, N.N. Inamdar, Chitosan modifications and applications: Opportunities galore, *React. Funct. Polym.* 68 (2008) 1013–1051.
- [17] M. Rinaudo, Chitin and chitosan: Properties and applications, *Prog. Polym. Sci.* 31 (2006) 603–632.
- [18] L. Zhou, Z. Liu, J. Liu, Q. Huang, Adsorption of Hg(II) from aqueous solution by ethylenediamine-modified magnetic crosslinking chitosan microspheres, *Desalination* 258 (2010) 41–47.
- [19] M. Monier, Adsorption of  $Hg^{2+}$ ,  $Cu^{2+}$  and  $Zn^{2+}$  ions from aqueous solution using formaldehyde cross-linked modified chitosan-thioglyceraldehyde Schiff's base, *Int. J. Biol. Macromol.* 50 (2012) 773–781.
- [20] S.T. Lee, F.L. Mi, Y.J. Shen, S.S. Shyu, Equilibrium and kinetic studies of copper(II) ion uptake by chitosan-tripolyphosphate chelating resin, *Polymer* 42 (2001) 1879–1892.
- [21] M.K. Sureshkumar, D. Das, M.B. Mallia, P.C. Gupta, Adsorption of uranium from aqueous solution using chitosan-tripolyphosphate (CTPP) beads, *J. Hazard Mater.* 184 (2010) 65–72.
- [22] B. Kannamb, K. Laxma Reddy, B.V. AppaRao, Removal of Cu(II) from aqueous solutions using chemically modified chitosan, *J. Hazard Mater.* 175 (2010) 939–948.
- [23] R.S. Vieira, M.M. Beppu, Interaction of natural and cross-linked chitosan membranes with Hg(II) ions, *Colloids Surf. A* 279 (2006) 196–207.
- [24] Y.K. Sun, M. Ma, Y. Zhang, N. Gu, Synthesis of nanometer-size maghemite particles from magnetite, *Colloids Surf. A Physicochem. Eng. Aspects* 245 (2004) 15–19.
- [25] T.S. West, *Complexometry with EDTA and Related Reagents*, third ed., BDH Chemicals Ltd., 1969.
- [26] A.M. Donia, A.A. Atia, K.Z. Elwakeel, Gold(III) recovery using synthetic chelating resins with amine, thio and amine/mercaptan functionalities, *Sep. Purif. Technol.* 42 (2005) 111–116.
- [27] P.K. Malik, Dye removal from wastewater using activated carbon developed from sawdust: Adsorption equilibrium and kinetics, *J. Hazard Mater.* 113 (2004) 81–88.
- [28] Y.S. Ho, G. McKay, Pseudo-second-order model for sorption processes, *Process Biochem.* 34 (1999) 451–465.
- [29] M. Sarkar, P. Acharya, B. Bhattacharya, Modeling the adsorption kinetics of some priority organic pollutants in water from diffusion and activation energy parameters, *Colloid Interf. Sci.* 266 (2003) 28–32.
- [30] E. Guibal, C. Milot, J.M. Tobin, Metal-anion sorption by chitosan beads: Equilibrium and kinetic studied, *Ind. Eng. Chem. Res.* 37 (1998) 1454–1463.
- [31] B. Ji, F. Shao, G. Hu, S. Zheng, Q. Zhang, Z. Xu, Adsorption of methyl tert-butylether (MTBE) from aqueous solution by porous polymeric adsorbents, *J. Hazard Mater.* 161 (2009) 81–87.
- [32] M. Dogan, H. Abak, M. Alkan, Adsorption of methylene blue onto hazelnut shell: Kinetics, mechanism and activation parameters, *J. Hazard Mater.* 164 (2009) 172–181.
- [33] B.H. Hameed, A.A. Ahmad, N. Aziz, Adsorption of reactive dye on palm-oil industry waste: Equilibrium kinetic and thermodynamic studies, *Desalination* 247 (2009) 551–560.
- [34] H.C. Chu, K.M. Chen, Reuse of activated sludge biomass: II. The rate processes for adsorption of basic dyes on biomass, *Process Biochem.* 37 (2002) 1129–1134.
- [35] A.E. Ofomaja, Intraparticle diffusion process for lead(II) biosorption onto mansonia wood sawdust, *Biores. Technol.* 101 (2010) 5868–5876.
- [36] S.S. Tahir, N. Rauf, Thermodynamic studies of Ni(II) sorption onto bentonite from aqueous solution, *J. Chem.* 35 (2003) 2003–2009.
- [37] J.G.P. Espinola, L.N.H. Arakaki, S.F. Oliveira, M.G. Fonseca, J.A.A.C. Filho, C. Airoidi, Some thermodynamic data of the energetics of the interaction cation-piperazine immobilized on silica gel, *Colloids Surf. A* 221 (2003) 101–108.
- [38] J.A.A. Sales, C. Airoidi, Calmetric investigation of metal ion adsorption on 3-glycidoxy-propyltrimethylsiloxanepropane-1,3-diamin immobilized on silica gel, *Thermochim. Acta* 427 (2005) 77–83.
- [39] K.M. Abd El-Rahman, M.R. El-Sourougy, Y.N.M. Abdel-Monem, I.M. Ismail, Modeling the sorption kinetics of cesium and strontium ion on zeolite, A, *J. Nucl. Radiochem. Sci.* 7 (2006) 21–27.
- [40] A.M. Donia, A.A. Atia, K.Z. Elwakeel, Recovery of gold(III) and silver(I) on a chemically modified chitosan with magnetic properties, *Hydrometallurgy* 87 (2007) 197–206.